Immunity
Article

CXCR3 Chemokine Receptor-Ligand Interactions in the Lymph Node Optimize CD4$^+$ T Helper 1 Cell Differentiation

Joanna R. Groom,[1,3] Jillian Richmond,[1] Thomas T. Murooka,[1] Elizabeth W. Sorensen,[1] Jung Hwan Sung,[2] Katherine Bankert,[1] Ulrich H. von Andrian,[2] James J. Moon,[1] Thorsten R. Mempel,[1] and Andrew D. Luster[1,*]
[1]Center for Immunology and Inflammatory Diseases, Division of Rheumatology, Allergy and Immunology, Massachusetts General Hospital, Harvard Medical School, Boston, MA 02114, USA
[2]Immune Disease Institute and Department of Microbiology & Immunology, Harvard Medical School, Boston, MA 02115, USA
[3]Present address: Department of Medical Biology, The Walter and Eliza Hall Institute of Medical Research, University of Melbourne, 1G Royal Parade, VIC 3052, Australia
*Correspondence: aluster@mgh.harvard.edu
http://dx.doi.org/10.1016/j.immuni.2012.08.016

SUMMARY

Differentiation of naive CD4$^+$ T cells into T helper (Th) cells is a defining event in adaptive immunity. The cytokines and transcription factors that control Th cell differentiation are understood, but it is not known how this process is orchestrated within lymph nodes (LNs). Here we have shown that the CXCR3 chemokine receptor was required for optimal generation of interferon-γ (IFN-γ)-secreting Th1 cells in vivo. By using a CXCR3 ligand reporter mouse, we found that stromal cells predominately expressed the chemokine ligand CXCL9 whereas hematopoietic cells expressed CXCL10 in LNs. Dendritic cell (DC)-derived CXCL10 facilitated T cell-DC interactions in LNs during T cell priming while both chemokines guided intranodal positioning of CD4$^+$ T cells to interfollicular and medullary zones. Thus, different chemokines acting on the same receptor can function locally to facilitate DC-T cell interactions and globally to influence intranodal positioning, and both functions contribute to Th1 cell differentiation.

INTRODUCTION

CD4$^+$ T cells play a central role in orchestrating adaptive immune responses. Naive CD4$^+$ T cells are activated in draining lymph nodes (dLNs) by cognate antigen-loaded dendritic cells (DCs) where they differentiate into one of several lineages of helper T cell subsets, such as T helper type 1 (Th1), Th2, Th17, T follicular helper (Tfh), and induced T regulatory (iTreg) cells (Zhu et al., 2010). For example, Th1 cells secrete interleukin-2 (IL-2), interferon-γ (IFN-γ), and tumor necrosis factor-α (TNF-α) and promote cellular immune responses mainly to intracellular pathogens and tumors. Differentiation into a particular helper subset is guided by extrinsic cytokine cues that induce lineage-specifying transcription factors. Although the cytokines and transcription factors that control this process are relatively well understood, far less is known about how this process is temporally and spatially orchestrated within dLNs in vivo, where it initially takes shape.

CD4$^+$ T cells require persistent antigen throughout their expansion to differentiate (Obst et al., 2005). Multiple successive phases of T cell priming have been described based on dynamic interactions between T cells and DCs in dLNs (Mempel et al., 2004; Miller et al., 2004). First, T cells sporadically interact with DCs, leading to an initial increase in T cell activation. Subsequently, T cells undergo sustained interactions with DCs, which are probably required to induce T helper cell differentiation. Diminished contact stability at this time leads to reduction in IFN-γ production in settings where Th1 cells are induced (Hugues, 2010). Finally, repeated engagements of DCs by the daughters of newly activated CD4$^+$ T cells may also be required to optimally differentiate into IFN-γ-producing Th1 cells (Celli et al., 2005; Itano et al., 2003).

The migration of priming T cells to different LN compartments during antigenic priming may expose T cells to different types of antigen-presenting cells (APCs) and provide them with unique differentiation cues. For instance, activated migratory and LN-resident DCs localize to different dLN regions, including the deep and the superficial paracortex, as well as the interfollicular T cell zones and medullary regions (Hickman et al., 2008; Itano et al., 2003; Tang and Cyster, 1999). In the course of this antigenic priming, T cells may redistribute to these peripheral regions of the LN, and once there may be exposed to other APC types or cytokine cues than those present in the deep paracortex (Hickman et al., 2008).

The induction of chemokine receptors is intertwined with CD4$^+$ T cell differentiation. The differentiation of a particular helper subset instructs the upregulation of a specific set of homing receptors, which guide effector cells out of the lymphoid compartment and into otherwise restricted peripheral sites of inflammation (Bromley et al., 2008). How chemokines participate in the process of Th cell differentiation is not known but there are two likely possibilities. First, DCs may use chemokines to promote encounters with antigen-specific T cells (Friedman et al., 2006; Molon et al., 2005). Second, chemokines expressed in specific LN regions may influence more globally the intranodal positioning of priming T cells to particular microenvironments, to bring these cells in contact with the appropriate APCs or accessory cells important for their differentiation (Tang and Cyster, 1999).

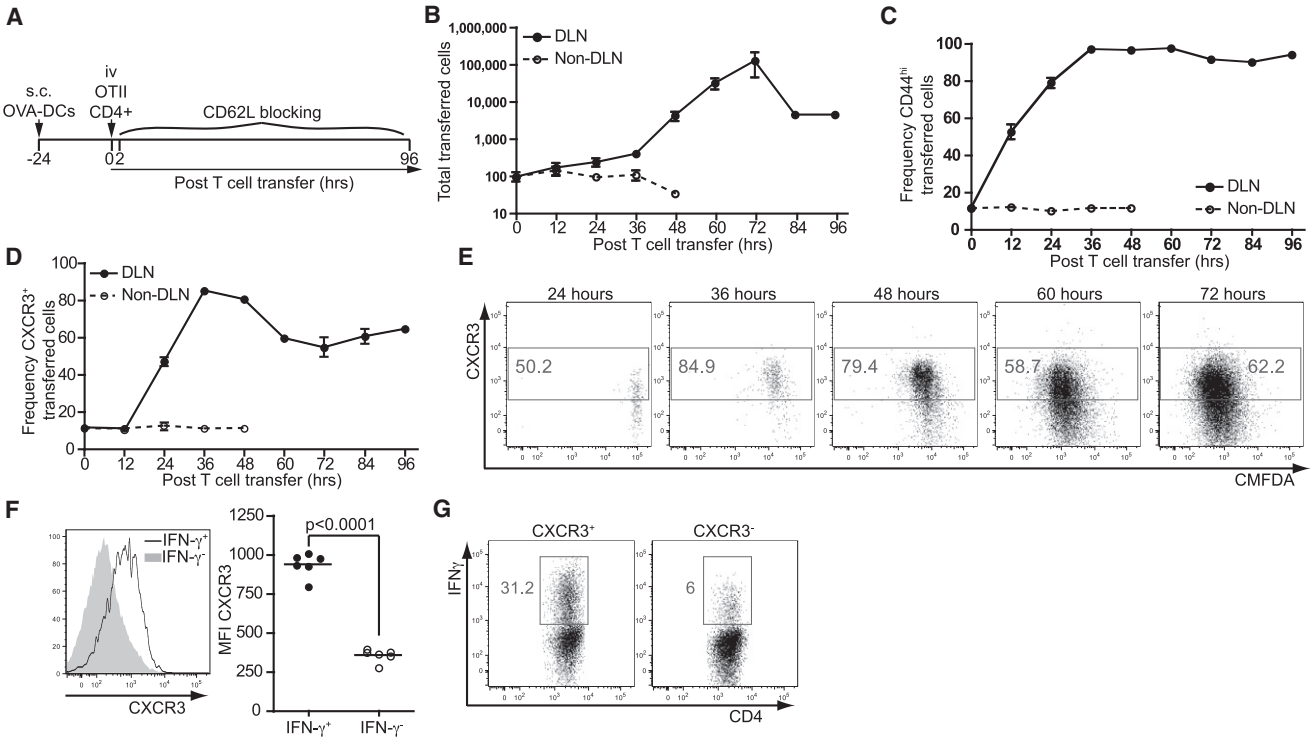

Figure 1. CXCR3 Expression Is Upregulated Rapidly in Draining LNs and Correlates with IFN-γ Expression

(A) Experimental protocol. Antigen-pulsed DCs were injected 24 hr before i.v. OT-II cells. (Phenotype of transferred DCs shown in Figure S1.) CD62L blocking antibody was given 2 hr after OT-II cell transfer and every 24 hr. At times indicated, dLNs (popliteal) and non-dLNs (bracial) were harvested to assess T cell activation.

(B–E) Time course of (B) cell numbers and of (C) CD44 and (D, E) CXCR3 cell surface induction on transferred OT-II cells.

(F and G) Correlation between IFN-γ^+ cells and CXCR3 mean fluorescence intensity (MFI). Data are representative of three independent experiments (n = 4–6). Error bars denote SEM.

CXCR3 is the receptor for the interferon-inducible chemokines CXCL9 (MIG), CXCL10 (IP-10), and CXCL11 (I-TAC). CXCR3 expression on activated T cells is important for the amplification of IFN-γ-dependent recruitment into peripheral sites of infection and autoimmune responses (Groom and Luster, 2011a). However, CXCR3 ligands are also expressed in dLNs during Th1 cell differentiation (Martín-Fontecha et al., 2004; Yoneyama et al., 2002).

We sought to determine the role of CXCR3 receptor-ligand interactions in $CD4^+$ T cell differentiation in dLNs by using two models of $CD4^+$ T cell priming to address the potential roles for this chemokine system described above: promoting DC-T cell interactions and intranodal positioning of T cells. The first model examined interactions of DCs and $CD4^+$ T cells in the LN that induce Th1 cell polarization. In this model, antigen-pulsed DCs were injected subcutaneously into the footpad of mice from where they migrate into dLNs and interact with cognate antigen-specific T cells (Ingulli et al., 1997; Miller et al., 2004). The second model examined the global positioning of $CD4^+$ T cell in the reactive LN required for optimal Th1 cell generation. Here, soluble antigen was introduced into peripheral tissue to mimic the physiological delivery of antigen to LNs via the lymph, where both migratory and resident DCs may influence T cell priming. To characterize chemokine expression in the dLNs, we developed a transgenic (Tg) mouse that reports the expression of both CXCL9 and CXCL10, called REX3 (reporting the expression of CXCR3 ligands). By using these in vivo models of immunization and REX3 Tg mice, we found that the CXCR3 system regulated the local interactions of antigen-specific $CD4^+$ T cell with cognate antigen-loaded DCs in the LN, as well as the global intranodal positioning of $CD4^+$ T cells after antigen-induced activation, both of which contribute to Th1 cell differentiation.

RESULTS

Rapid Upregulation of CXCR3 in $CD4^+$ T Cells Correlates with IFN-γ Production

To study the in vivo development of Th1 cells, we first outlined the kinetics of CXCR3 upregulation by antigen-specific $CD4^+$ T cells in LNs by using a controlled activated LN reaction (Figure 1A). Expanded DCs were pulsed with ovalbumin (OVA) protein activated with lipopolysaccharide (LPS) and poly(I:C) (Figure S1B available online) and subcutaneously transferred into the footpads of naive mice. Purified $CD11c^+MHC\text{-}II^{hi}$ DCs contained both $CD8^+$ and $CD11b^+$ subpopulations; however, only $CD11b^+$ cells successfully migrated to the LN (Figures S1A and S1C). At 24 hr after DC injections, mice were given naive OVA-specific $CD4^+$ T cells isolated from OT-II Tg mice. At 2 hr after T cell transfer, CD62L blocking antibody was given to

synchronize T cell activation by inhibiting further entry into dLNs (Mempel et al., 2004). After T cell transfer, the dLNs were harvested and OT-II cells were assessed for accumulation, proliferation, and expression of CD44 and CXCR3. Although slower than CD44 upregulation, the initially low CXCR3 expression was upregulated within 24 hr after T cell transfer, prior to T cell proliferation (Figures 1B–1E). After the first cycles of proliferation, $CXCR3^+$ cells peaked, with the majority of OT-II cells expressing CXCR3 (Figures 1D and 1E). The frequency of $CXCR3^+$ cells then decreased slightly but remained above 50% throughout the activated LN reaction prior to cells leaving the LN (Figures 1B and 1D). IFN-γ production peaked in this model at 60 hr (Figures S1D and S1E). At this time, cells producing IFN-γ had a higher mean fluorescence intensity (MFI) of CXCR3 expression than did cells that failed to produce cytokine, and cells expressing CXCR3 were more likely to be IFN-γ producers (Figures 1F and 1G). Thus, CXCR3 is upregulated and remains high on antigen-specific T cells in dLNs and correlates with their production of IFN-γ.

CXCR3 Is Required for Optimal Th1 Cell-Associated Cytokine Production and Activation of OT-II Cells

CXCR3 and its ligands play an important role in the trafficking of effector Th1 $CD4^+$ cells into inflamed peripheral tissues. However, CXCR3 is upregulated in dLNs well before T cell egress (Figure 1). Whether CXCR3 also influences the generation of Th1 cells is unknown. To investigate this, we cotransferred WT and *Cxcr3*$^{-/-}$ OT-II cells after DC injection. At 60 hr after T cell transfer, the frequency of IFN-γ-producing *Cxcr3*$^{-/-}$ OT-II cells was reduced by ~50% compared to WT OT-II cells (Figures 2A and 2B). A less pronounced but significant reduction was observed for IL-2 and TNF-α. Because no difference was seen in the overall numbers of WT and *Cxcr3*$^{-/-}$ cells in the dLN, this decrease in cytokine-producing cells translated into a decrease in the total number of polyfunctional (cells producing IL-2, TNF-α, and IFN-γ) OT-II cells (Figure 2C). *Cxcr3*$^{-/-}$ OT-II cells also displayed markedly lower surface activation markers CD25, CD40L (CD152), and CD69 than did cotransferred WT OT-II cells (Figure 2D).

To address whether the decrease in IFN-γ^+ cells seen in the *Cxcr3*$^{-/-}$ population was due to competition for interactions with DCs, naive WT or *Cxcr3*$^{-/-}$ OT-II cells were transferred into separate DC-injected hosts and assessed for effector cytokine production. In this noncompetitive setting, *Cxcr3*$^{-/-}$ OT-II cells displayed the same reduced frequency of IFN-γ^+TNF-α^+ cells as seen in the cotransfer experiments (Figures S2A and S2B).

To eliminate the requirement for cells to migrate toward OVA-pulsed DCs, WT and *Cxcr3*$^{-/-}$ OT-II cells were cocultured and differentiated in vitro. In these conditions, the cells producing IFN-γ were evenly split between the T cells of each genotype (Figure S2C), indicating that there was a unique requirement for *Cxcr3* expression in vivo. Although the numbers of WT and *Cxcr3*$^{-/-}$ OT-II cells present in the dLNs was comparable, a possible defect in proliferation could account for decreased production of polyfunctional Th1 cells in the *Cxcr3*$^{-/-}$ OT-II cells. However, carboxymethyl fluorescein diacetate (CMFDA) dilution profiles of WT and *Cxcr3*$^{-/-}$ OT-II cells were overlapping 60 hr after T cell transfer, when cell entry into the LN was or was not blocked with CD62L antibody treatment (Figure 2E). To ensure that differences in IFN-γ^+ production by *Cxcr3*$^{-/-}$ OT-II cells were not due to differences in their egress from dLNs into peripheral tissues (Yoneyama et al., 2002), mice were either left untreated, treated with CD62L blocking antibody as above, or treated with both CD62L antibody and FTY720, which induces the sequestration of T cells in lymphoid organs by modulating $S1P_1$ and inhibiting LN T cell egress (Matloubian et al., 2004). Neither blocking T cell egress nor allowing continued T cell entry into dLNs altered the decrease in effector cytokine production seen in *Cxcr3*$^{-/-}$ cells compared to WT OT-II cells (Figure 2F). Finally, we performed a kinetic experiment of IFN-γ production. Although the maximum frequency of IFN-γ-producing cells varied throughout analysis (Figures S1D and S1E), at each time point cotransferred *Cxcr3*$^{-/-}$ cells demonstrated a similar decrease in IFN-γ production compared to WT OT-II cells (Figure 2G). Collectively, these data show that CXCR3 expression is important for optimizing Th1 $CD4^+$ cell responses. This effect was not observed in vitro and was not related to proliferation, different kinetics of IFN-γ expression, or early egress of *Cxcr3*$^{-/-}$ T cells from LNs.

Both CXCR3 Ligands Are Induced in dLNs during Th1 Cell Differentiation

Given the role for CXCR3 on $CD4^+$ T cells during their differentiation to Th1 effector cells, we investigated the expression of CXCR3 ligands during inflammatory LN reactions. We focused on the CXCR3 ligands CXCL9 and CXCL10, because the third CXCR3 ligand, CXCL11, is not expressed in C57BL/6 mice at the protein level as demonstrated by immunoblot (Figures S3A and S3B) as a result of a frame shift mutation (Sierro et al., 2007). To examine the expression of CXCR3 ligands at times relevant to Th1 cell differentiation, we first examined the upregulation of *Cxcl9* and *Cxcl10* by RNA analysis of whole draining and nondraining LNs during our activated DC transfer LN model. Both ligands were highly upregulated in dLNs, whereas they remained minimally expressed in non-dLNs (Figures S3C and S3D).

CXCL10 Expression by Antigen-Presenting DCs Is Important for Th1 Cell Differentiation

CXCL9 and CXCL10 have been observed in various models to display overlapping as well as unique functions (Groom and Luster, 2011b). In this regard, it has been unclear which, if any, of the CXCR3 ligands is the major contributor toward promotion of Th1 cell differentiation. Expanded WT, *Cxcl9*$^{-/-}$, and *Cxcl10*$^{-/-}$ DCs were pulsed and activated as described above and injected into naive mice. At 60 hr after OT-II T cell transfer, DCs expanded from *Cxcl10*$^{-/-}$ cells were not capable of supporting the induction of IFN-γ^+TNF-α^+-producing OT-II cells. In contrast, *Cxcl9*$^{-/-}$ DCs were as capable as WT DCs in inducing IFN-γ^+TNF-α^+-producing OT-II cells (Figures 3A and 3B). Of note, OT-II T cell IFN-γ production in mice receiving *Cxcl10*$^{-/-}$ DCs was reduced to a greater degree than *Cxcr3*$^{-/-}$ T cells cotransferred with WT T cells (Figure 2). This may be due to an additional influence of DC-derived CXCL10 on host accessory cells such as natural killer (NK) cells and plasmacytoid dendritic cells (pDCs), which express CXCR3 and are known to influence Th1 cell differentiation (Martín-Fontecha et al., 2004; Yoneyama et al., 2004). To eliminate other intrinsic defects in *Cxcl10*$^{-/-}$

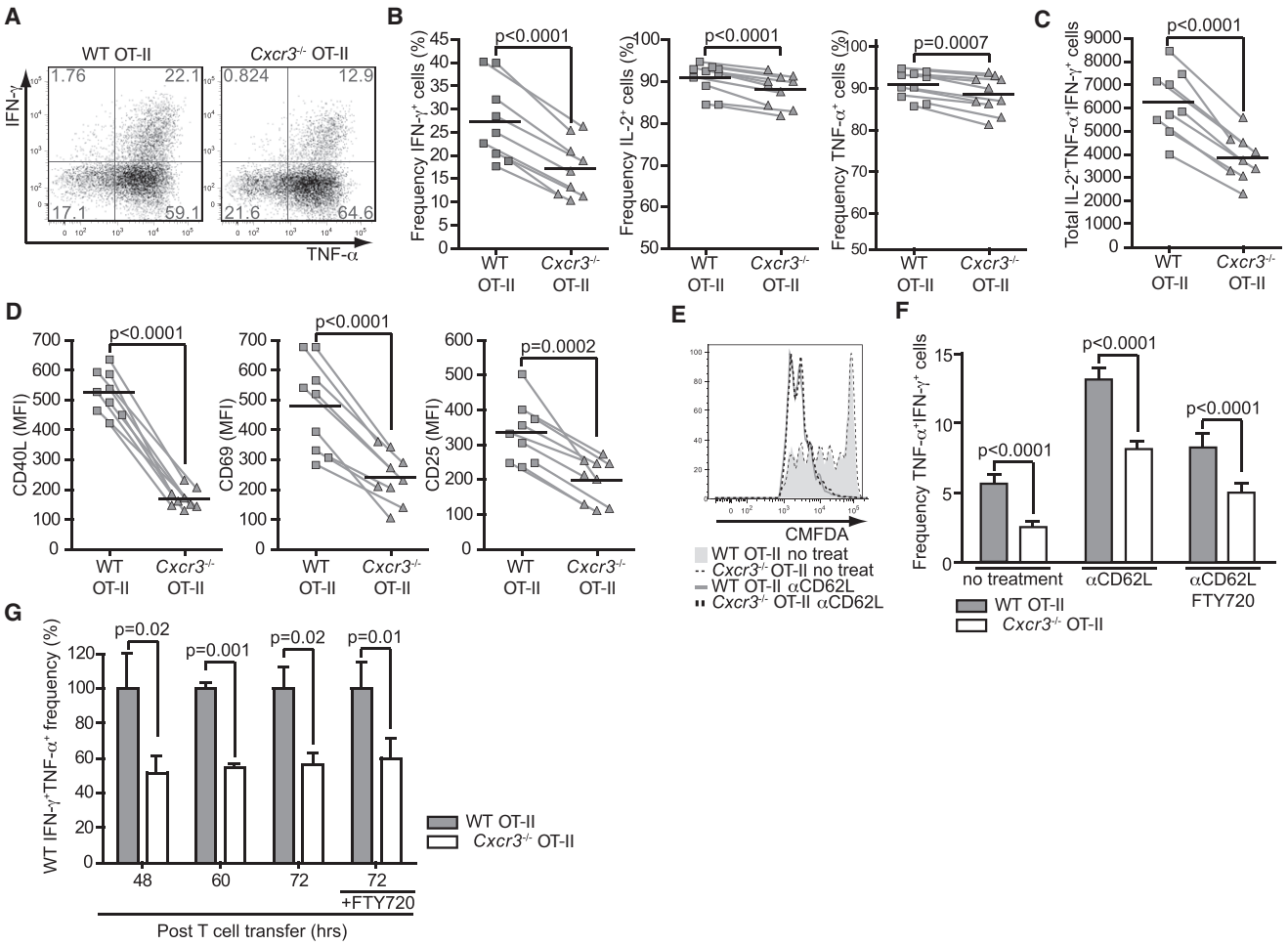

Figure 2. CXCR3 Is Required for Optimal Th1 Cell Differentiation after Transfer of OVA-Pulsed DCs

WT and *Cxcr3*$^{-/-}$ OT-II cells were cotransferred into WT hosts that received OVA-pulsed DCs. 60 hr after T cell transfer, dLNs were harvested.

(A) Plots of IFN-γ and TNF-α production by WT and *Cxcr3*$^{-/-}$ OT-II cells.

(B) Frequency of IFN-γ$^+$, IL-2$^+$, TNF-α$^+$ WT (square) and *Cxcr3*$^{-/-}$ (triangle) OT-II cells.

(C) Total numbers of polyfunctional (producing IL-2, TNF-α, and IFN-γ) WT and *Cxcr3*$^{-/-}$ OT-II cells in dLNs.

(D) MFI of CD40L, CD69, CD25 at 24–36 hr after T cell transfer of WT and *Cxcr3*$^{-/-}$ OT-II cells.

(B–D) Lines connect paired WT and *Cxcr3*$^{-/-}$ OT-II cells transferred into the same WT host.

(E) CMFDA labeled cell proliferation after WT (gray) and *Cxcr3*$^{-/-}$ (dashed) OT-II cell cotransfer. No treat mice (without CD62L blocking) were included to show peaks with continual T cell entry.

(F) Frequency of TNF-α$^+$IFN-γ$^+$ WT (gray) and *Cxcr3*$^{-/-}$ (open) OT-II cells in mice without or with CD62L blocking alone or with FTY720.

(G) Kinetics of WT and *Cxcr3*$^{-/-}$ OT-II cell induction of IFN-γ$^+$TNF-α$^+$.

Data are representative of three independent experiments (n = 6–8). Error bars denote SD. See Figures S2A and S2B for transfer of WT and *Cxcr3*$^{-/-}$ cells into separate hosts and Figure S2C for in vitro polarization of WT and *Cxcr3*$^{-/-}$ OT-II cells.

DCs, we determined that these cells were capable of migrating to dLNs and facilitating the early upregulation of CD25 on OT-II cells in vivo and inducing IFN-γ production in vitro to the same degree as WT and *Cxcl9*$^{-/-}$ DCs (Figures S3E–S3G).

Generation of REX3 Transgenic Mice

Although RNA analysis of whole dLNs (Figures S3C and S3D) established that CXCL9 and CXCL10 are expressed at times relevant to Th1 cell differentiation in vivo, it offered little information on the precise timing, location, and cell types expressing these ligands. Therefore, we generated a reporter mouse in which spectrally distinct fluorescent reporter proteins (FPs) report the RNA expression of the CXCR3 ligands *Cxcl9* and *Cxcl10*. To allow reporting of the expression of CXCR3 ligands (REX3) Tg mice, we inserted red fluorescent protein (RFP) at the start codon of *Cxcl9* and inserted blue fluorescent protein (BFP) at the start codon of *Cxcl10* in a CXCR3-ligand-containing bacterial artificial chromosome (BAC) (Figures 3C and S3H). Accurate reporting of *Cxcl9* and *Cxcl10* expression was confirmed by correlating the induction of RNA transcripts and protein with induction of FPs in stimulated REX3 Tg DCs (Figures S3J–S3L). CXCL9 immunostaining in REX3 Tg dLNs correlated with the expression of the CXCL9-RFP reporter, indicating that most of the chemokine protein detected is presented

by cells producing it and not dispersed throughout the LN (Figure S3M).

Chemokine-Expressing DCs Display Increased Activation

To visualize the expression of CXCL9 and CXCL10 by transferred, antigen-presenting DCs throughout the inflamed LN model, REX3 Tg DCs were pulsed with antigen, activated, and CMFDA labeled prior to subcutaneous footpad injections into WT mice. CMFDA$^+$ DCs were then tracked to assess reporter expression (Figure 3D). The majority of transferred DCs expressed both CXCL9-RFP and CXCL10-BFP within 12 hr of T cell transfer. In addition, smaller populations of CXCL10-BFP single expressers and double-negative DCs were detected, but single-positive CXCL9-RFP DCs were never observed. The frequency of cells in each of these populations remained stable throughout the time course (Figure 3D). We assessed whether there were any activation differences between DCs expressing REX3$^+$ FPs and those without expression. Although no difference was seen in expression of major histocompatibility complex (MHC) class II between these populations, REX3^{++} DCs (dually expressing CXCL9-RFP and CXCL10-BFP) had increased expression of the activation markers CD40 and CD86 compared to DCs without reporter expression (Figure 3E). Thus, identifying chemokine reporter cells allowed us to observe that both CXCL9 and CXCL10 are expressed by DCs at times relevant to Th1 cell differentiation and that this expression correlates with increased activation of APCs.

Cxcr3$^{-/-}$ OT-II Cells Display Altered Behavior in dLNs during CD4$^+$ T Cell Priming

In vitro, production of CXCR3 ligands by DCs enhances their ability to attract T cells (Padovan et al., 2002). We therefore tested whether this might be relevant in vivo. The use of multiphoton microscopy (MP-IVM) has revealed that the duration of T cell-DC interactions correlates with efficient T cell priming and IFN-γ production (Hugues, 2010). To gain insight into why *Cxcr3*$^{-/-}$ OT-II CD4$^+$ T cells do not optimally differentiate into Th1 cells, we characterized their in vivo movements via MP-IVM. When draining popliteal LNs were surgically exposed, transferred REX3 Tg DCs could be visualized. However, CXCL9-reporting RFP photo-bleached rapidly, leading to visualization of transferred DCs solely through BFP expression in time-lapse recording. At 6 to 8 hr after i.v. cotransfer of labeled WT and *Cxcr3*$^{-/-}$ OT-II T cells, both populations were capable of forming stable contacts with DCs (Figures 3F and 3H). However, although WT cells were almost uniformly engaged in stable contacts, as reflected by low migratory velocity, low confinement ratio, and high arrest coefficients (Figure 3G), a 3- to 4-fold larger fraction (~30%) of *Cxcr3*$^{-/-}$ cells compared to WT cells failed to form long-lasting interactions (Figure 3G). Even 24 hr after transfer, when both T cell populations had resumed motile behavior, *Cxcr3*$^{-/-}$ OT-II cells were less confined in their migration (Figure S4). Analysis of the contacts of T cells with CXCL10-BFP-expressing DCs showed that the majority of *Cxcr3*$^{-/-}$ OT-II cells did not visibly engage with these cells (Figures 3H and 3I). When the length of short-lived DC-T cell interactions was assessed, contact times of *Cxcr3*$^{-/-}$ OT-II cells with REX3$^+$ DCs were indeed shorter than those of WT OT-II cells (Figures 3F, 3H, and 3I). Combined, data generated by transfer of antigen-pulsed DCs established that *Cxcr3*$^{-/-}$ CD4$^+$ cells cannot maximally differentiate into IFN-γ^+ Th1 cells, which correlated with their reduced ability to interact with CXCL10-expressing antigen-presenting DCs.

Immunization Requires CXCR3 for Optimal Th1 Cell Differentiation

Thus far, our results addressed the requirement for CXCR3 ligands produced by CD11b$^+$ antigen-presenting DCs in the dLN; however, CXCL9 and CXCL10 are expressed by multiple hematopoietic and stromal cells residing within dLNs (Gattass et al., 1994; Martín-Fontecha et al., 2004). We therefore investigated whether chemokines produced by these cells were also important for optimal Th1 cell responses, reasoning that immunization with soluble antigen may correlate more with vaccination strategies than the transfer of antigen-pulsed DCs. For these studies, naive host mice were immunized with OVA protein with LPS and poly(I:C) subcutaneously. After 24 hr, mice were cotransferred with naive WT and *Cxcr3*$^{-/-}$ OT-II cells, which were assessed for the production of IFN-γ and TNF-α 60 hr after T cell transfer (Figure 4A). As seen with transferred antigen-pulsed DCs (Figure 2), after immunization with soluble antigen, CXCR3 ligand-receptor interactions were required for optimal differentiation of OT-II cells toward a Th1 cell phenotype (Figures 4B–4D).

We next used REX3 Tg mice as hosts in this model to identify the pattern of expression of CXCL9 and CXCL10 in dLNs. In unimmunized REX3 Tg mice, popliteal LNs showed little expression of either CXCL9-RFP or CXCL10-BFP (Figure 4E). However, during the inflamed LN reaction, expression was greatly increased, peaking at 24–36 hr after T cell transfer, before declining again at 60 hr (Figure 4F). Surprisingly, although some double-positive staining was observed, it appeared that CXCL9 and CXCL10 had strikingly different expression patterns. CXCL10 was primarily expressed in the LN medulla, the site into which the most of the lymph and lymph-borne antigens drain. Meanwhile, the strongest CXCL9-RFP expression was seen in interfollicular areas. These areas serve as transit corridors for lymphocytes migrating into and out of T cell areas and are also areas where T cells may survey DCs. In contrast, only scattered single- and dual-expressing cells for each chemokine were seen in the T cell zone where T cell-DC interactions are traditionally thought to occur (Figure 4F; Ingulli et al., 1997; Tang and Cyster, 1999). During the time course undertaken, there was minimal expression of either CXCR3 ligand inside B cell follicles (Figure 4F). These expression data from the REX3 Tg mice suggest the development of dramatic chemokine gradients in different regions of dLNs after immunization.

Nonredundant Roles for CXCL9 and CXCL10 in Th1 Cell Differentiation after Immunization

To investigate the patterns of chemokine expression further, we examined BM chimeras with REX3 Tg BM being transferred into irradiated WT hosts or vice versa. Strikingly, the majority of CXCL10-BFP expression was in the BM-derived hematopoietic compartment (Figure 5A). In contrast, CXCL9-RFP was

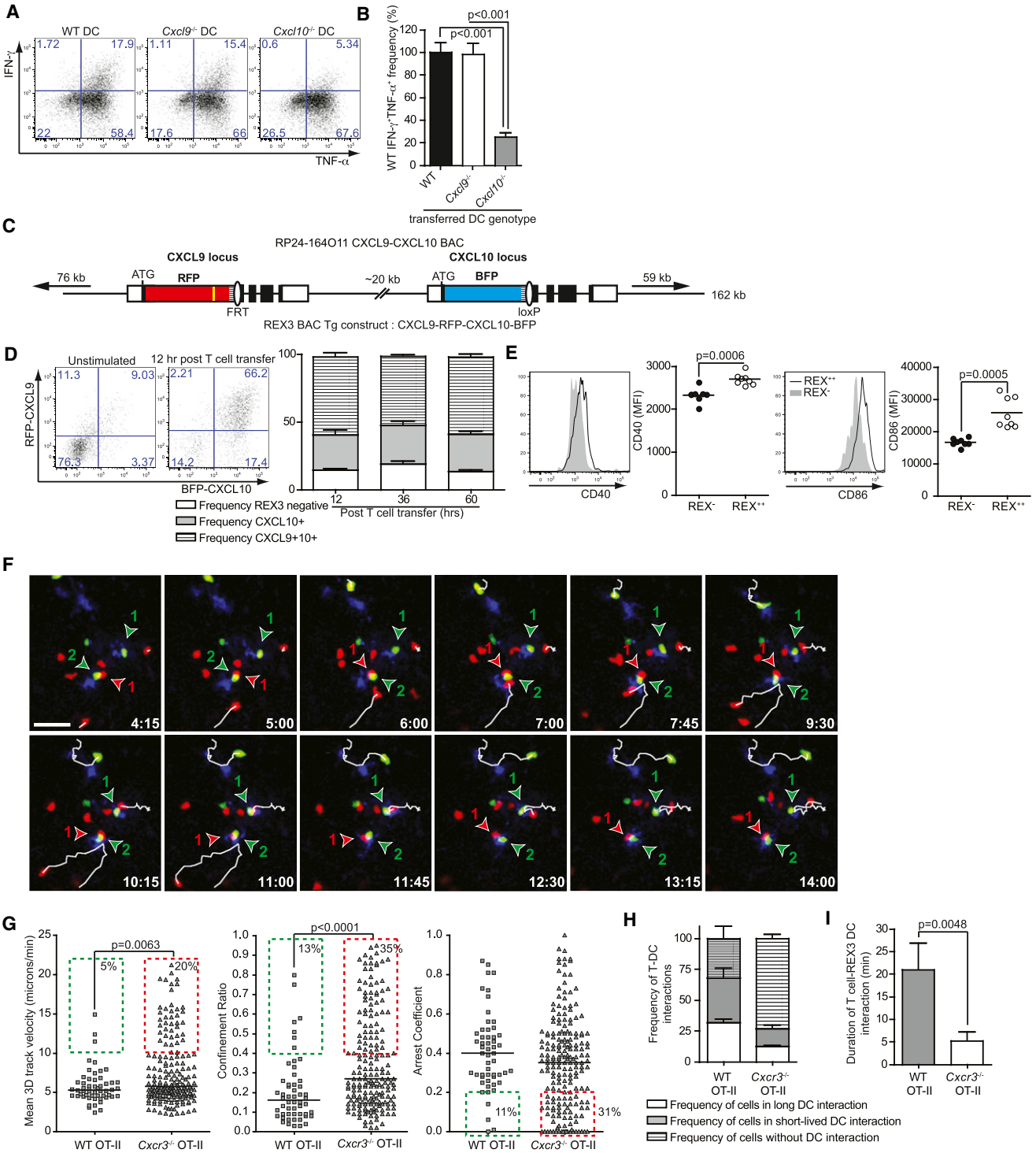

Figure 3. DC-Derived CXCL10 Optimizes Th1 Cell Responses and Identification of Chemokine-Expressing DCs during T Cell Priming

(A and B) Pulsed WT, *Cxcl9*$^{-/-}$, and *Cxcl10*$^{-/-}$ DCs were transferred to hosts prior to OT-II T cells. 60 hr after T cell transfer, dLN T cells were harvested.

(A) Plots of IFN-γ and TNF-α production of WT OT-II cells activated by DCs of indicated genotype.

(B) Frequency of TNF-α^{+}IFN-γ^{+} WT OT-II cells activated by WT (black), *Cxcl9*$^{-/-}$ (open), or *Cxcl10*$^{-/-}$ (gray) DCs.

(C) Schematic of REX3 Tg construct indicating insertion of RFP into the *Cxcl9* locus and BFP into the *Cxcl10* locus of the RP-24-164O11 BAC. Open box, noncoding exons; black box, coding exons of *Cxcl9* and *Cxcl10* genes; red box, RFP ORF; blue box, BFP ORF; striped box, SV40 poly(A) site; FRT Flippase Recognition Target and loxP Cre recombinase site.

(D) CMFDA-labeled DCs expanded from REX3 Tg were pulsed, stimulated, and injected into WT mice. Plot and bar graph indicating frequency of REX3-negative (open), CXCL10-BFP only (gray), and CXCL10-BFP and CXCL9-RFP double-positive (stripe) DCs.

predominantly expressed by the radio-resistant stromal cells located in the interfollicular and medulla areas of the dLN (Figure 5B).

We next assessed the role of each chemokine in CD4$^+$ T cell responses by using ligand-deficient mice after immunization. Surprisingly, both CXCL9 and CXCL10 were nonredundantly required for optimal Th1 cell differentiation after immunization (Figures 5C and 5D). This was in contrast to the DC transfer model, where only CXCL10-expressing antigen-pulsed DCs were required for maximal Th1 cell differentiation (Figures 3A and 3B). To determine which compartment was primarily required for maximum induction of Th1 cell differentiation, given the difference in expression of CXCL9 and CXCL10 seen in REX3 Tg BM chimeras, we immunized BM chimeric mice generated with WT, *Cxcl9*$^{-/-}$, or *Cxcl10*$^{-/-}$ BM transplanted into irradiated WT mice. WT host mice reconstituted with *Cxcl10*$^{-/-}$ BM showed a defect in Th1 cell differentiation, whereas mice containing WT stromal cells with *Cxcl9*$^{-/-}$ hematopoietic cells were capable of maximal induction of IFN-γ^+TNF-α^+ cells (Figure 5E). Finally, we performed BM chimera experiments where WT BM was used to reconstitute irradiated WT, *Cxcl9*$^{-/-}$, or *Cxcl10*$^{-/-}$ mice. In this setting, mice lacking either stromal-derived CXCL9 or CXCL10 displayed reduced numbers of IFN-γ^+TNF-α^+ T cells (Figure 5F). These data correlate with the expression data (Figures 5A and 5B) and demonstrate that CXCL10 produced by the hematopoietic compartment is critical, and both CXCL9 and CXCL10 produced by stromal cells are important.

CXCL9 and CXCL10 Gradients Promote Peripheralization of T Cells in the LN

Because the majority of chemokine-expressing cells were located peripheral to the T cell zone, we asked whether, after immunization, antigen-specific CD4$^+$ T cells migrate out of the T cell zone toward these areas in a CXCR3-dependent manner. We therefore investigated the intranodal location of WT and *Cxcr3*$^{-/-}$ OT-II cells in the T cell zone, interfollicular zone surrounding B cell follicles, or in the LN medulla (as described in Figure S5) before and after immunization. In unimmunized mice receiving either WT or *Cxcr3*$^{-/-}$ OT-II cells, transferred cells were predominantly located in the T cell zone (Figure 6A). In immunized hosts, 24–36 hr after T cell transfer, WT cells were located in the interfollicular and medulla regions, whereas the majority of *Cxcr3*$^{-/-}$ OT-II cells remained in the T cell zone (Figure 6A). Again, in unimmunized mice, cotransferred WT and *Cxcr3*$^{-/-}$ OT-II cells were similarly located in the T cell zone. After immunization, compared to *Cxcr3*$^{-/-}$ OT-II cells, WT OT-II cells had a greater propensity to move into the periphery of the dLN, where CXCR3 ligands were highly expressed (Figures 6B, 6C, and 4F). We next investigated the localization of WT OT-II cells in immunized WT, *Cxcl9*$^{-/-}$, or *Cxcl10*$^{-/-}$ hosts. WT OT-II cells were similarly located in the T cell zone in unimmunized WT, *Cxcl9*$^{-/-}$, and *Cxcl10*$^{-/-}$ hosts (Figures 6D and 6E). At 24–36 hr after T cell transfer into immunized hosts, WT OT-II cells in WT hosts migrated from the T cell zone into the peripheral regions of the dLN (Figures 6D and 6E). However, WT OT-II cells transferred into *Cxcl9*$^{-/-}$ hosts remained in the T cell zone, but showed some migration toward the medullary region, where predominantly CXCL10 was induced (Figures 6D, 6E, and 4F). WT OT-II cells transferred into *Cxcl10*$^{-/-}$ hosts also remained in the T cell zone, but conversely showed some migration toward the interfollicular areas of the dLN, where predominantly CXCL9 was induced (Figures 6D, 6E, and 4F). Combined, these data highlight the importance of intranodal migration during Th1 cell responses and the requirement for CXCR3 ligands, expressed by hematopoietic and stromal cells, in directing movement of T cells out of the T cell zone of dLNs for maximal Th1 cell differentiation.

CXCR3 Receptor-Ligand Interactions Promote Th1 Cell Differentiation in Response to Viral Infection

Although the DC transfer and immunization protocols outlined above allow for the discrimination of factors important for the differentiation of Th1 cells during a synchronized T cell response, it remained to be determined whether these mechanisms are relevant during a response to an intracellular pathogen, such as lymphocytic choriomeningitis virus (LCMV), that induces a strong Th1 cell-type immune response (Varga and Welsh, 2000). To address this, we evaluated the endogenous antigen-specific CD4$^+$ T cell response in WT, *Cxcl9*$^{-/-}$, *Cxcl10*$^{-/-}$, or *Cxcr3*$^{-/-}$ mice at the peak of acute LCMV infection. T cells responding to the dominant CD4$^+$ T cell epitope for LCMV were detected with MHC II-restricted gp66 tetramers (Figure 7A; Moon et al., 2011; Oxenius et al., 1995). Within the gp66^{tet+}CD44$^+$

(E) Tracked REX3^{++} (expressing CXCL10-BFP and CXCL9-RFP) and REX3$^-$ (REX3-negative) DCs MFI of CD40, CD86 at 24–36 hr after OT-II cell transfer. Histogram and MFI plots are shown.

(F–I) DCs expanded from REX3 Tg mice injected in WT mice. 24 hr later, WT and *Cxcr3*$^{-/-}$ OT-II cells were transferred i.v. MP-IVM of exposed dLN was performed at 6–8 hr after T cell transfer.

(F) Representative multiphoton intravital microcopy recording of REX3$^+$ DC interactions with WT and *Cxcr3*$^{-/-}$ OT-II cells. Numbered arrowheads indicate long-lived interactions between REX3$^+$ DCs and WT (green) or *Cxcr3*$^{-/-}$ (red) OT-II cells. White lines indicate tracks of WT and *Cxcr3*$^{-/-}$ cell centroids engaging in short-lived interactions with REX3$^+$ DCs. Elapsed time in minutes:seconds. Scale bar represents 30 μm.

(G) Mean 3D track velocity, confinement ratio, and arrest coefficient of WT and *Cxcr3*$^{-/-}$ OT-II cells. Dashed boxes around WT (green) and *Cxcr3*$^{-/-}$ (red) OT-II cells indicate the frequency of cells in the specified region; 3D track velocity > 10 μm/min; confinement ratio > 0.4; arrest coefficient < 0.2 (not arrested).

(H) Frequency of WT and *Cxcr3*$^{-/-}$ OT-II cells in long-term (open), short-lived (gray), or without (stripe) DC interactions.

(I) Short-lived interactions between REX3$^+$ DCs and either WT or *Cxcr3*$^{-/-}$ OT-II cells. Duration of contacts from movies imaged 6–8 hr after T cell transfer. Only interactions where the initiation and termination of the interactions were observed were analyzed.

Data are representative of three independent experiments (n = 3–6). Error bars denote SD. See Figures S3A and S3B for confirmation that C57BL/6 mice do not produce CXCL11 protein; Figures S3C and S3D for RNA expression of *Cxcl9* and *Cxcl10* in whole dLN or non-dLNs in mice receiving OT-II cells or not; Figures S3E–S3G for confirmation of *Cxcl10*$^{-/-}$ DC tracking and function; Figures S3H and S3I for BAC Tg construction and PCR genotyping of REX3 Tg mice; Figures S3J–S3M and Movie S1 for representative imaging performed 6–8 hr after T cell transfer; and Figure S4 for quantification of imaging performed at 24–27 hr after T cell transfer.

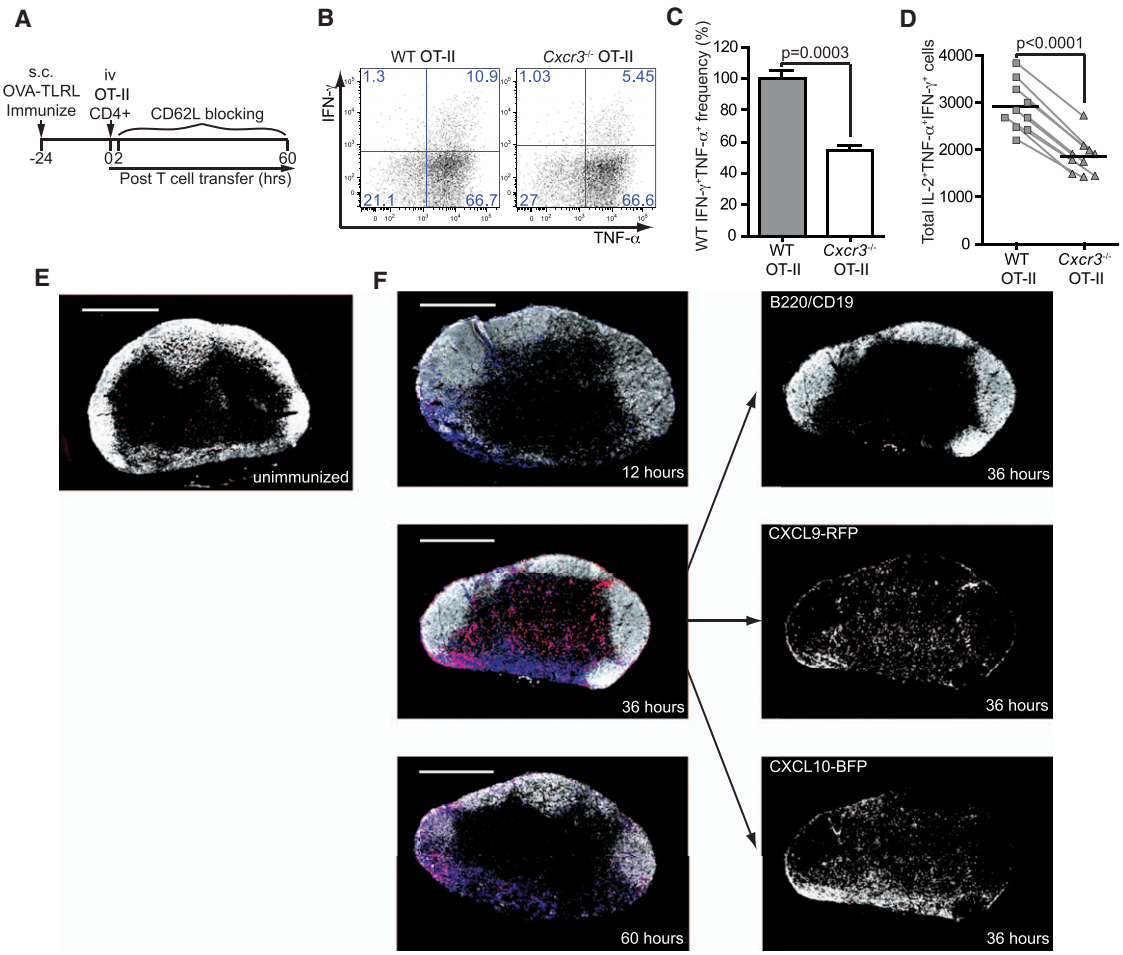

Figure 4. CXCR3 Is Required for Optimal Th1 Cell Differentiation after OVA and TLR-Ligand Immunization

(A) Experimental protocol. Host mice were immunized with OVA and LPS and poly(I:C) prior to i.v. cotransfer of WT and *Cxcr3*$^{-/-}$ OT-II cells. CD62L blocking antibody 2 hr after OT-II cell. 60 hr after T cell transfer, dLN T cells were harvested to assess cytokine production.

(B and C) Plots (B) and fold change (C) of IFN-γ and TNF-α production by WT and *Cxcr3*$^{-/-}$ OT-II cells.

(D) Total numbers of polyfunctional (producing IL-2, TNF-α, and IFN-γ) WT and *Cxcr3*$^{-/-}$ OT-II cells in dLNs. Lines connect paired WT and *Cxcr3*$^{-/-}$ OT-II cells transferred into the same WT host.

(E and F) LN sections from REX3 Tg mice. CXCL9-RFP, red; CXCL10-BFP, blue; B220 and CD19 immunostaining, white. Scale bars represent 500 μm.

(E) Unimmunized REX3 Tg LN.

(F) REX3 Tg dLNs after immunization. Right panels shows gray scale of B220 and CD19 immunostaining (top), CXCL9-RFP (middle), and CXCL10-BFP (bottom) of LN harvested at 36 hr after T cell transfer.

Data are representative of three independent experiments (n = 3–6). Error bars denote SD.

population, the frequency of IFN-γ$^+$TNF-α$^+$ cells was determined. Endogenous LCMV-specific CD4$^+$ T cells in *Cxcl9*$^{-/-}$ and *Cxcl10*$^{-/-}$ mice displayed a deficiency in maximal Th1 cell differentiation (Figures 7B and 7C). IFN-γ production by gp66^{tet+} CD44$^+$ cells in *Cxcr3*$^{-/-}$ mice was even further reduced, suggesting that CXCR3 was required on cells other than CD4$^+$ for Th1 cell responses. To determine the importance of CXCR3 exclusively on CD4$^+$ cells, the frequency of IFN-γ$^+$TNF-α$^+$ cells after LCMV infection was examined in mixed BM chimeras where WT and *Cxcr3*$^{-/-}$ BM was used to reconstitute irradiated *Rag1*$^{-/-}$ mice. Again, *Cxcr3*$^{-/-}$ antigen-specific CD4$^+$ T cells displayed a reduced frequency of IFN-γ production, compared to WT cells in the same hosts (Figures 7D and 7E). Together, these data validate our immunization models, indicating that CXCR3 receptor-ligand interactions optimizes Th1 cell differentiation during a response to a natural infectious pathogen.

DISCUSSION

The differentiation of naive CD4$^+$ T cells into Th cell subsets in LNs draining sites of infection and inflammation determines the type (e.g., Th1, Th2, Th17) of immune response that a pathogen or foreign antigen will elicit. We chose to study the CXCR3 chemokine system in Th1 cell development because of all the chemokine receptors, CXCR3 is most associated with Th1 cells (Groom and Luster, 2011a). Expression of CXCR3 by newly activated CD4$^+$ T cells correlated with their ability to produce IFN-γ and was required for optimal effector cytokine responses. Our

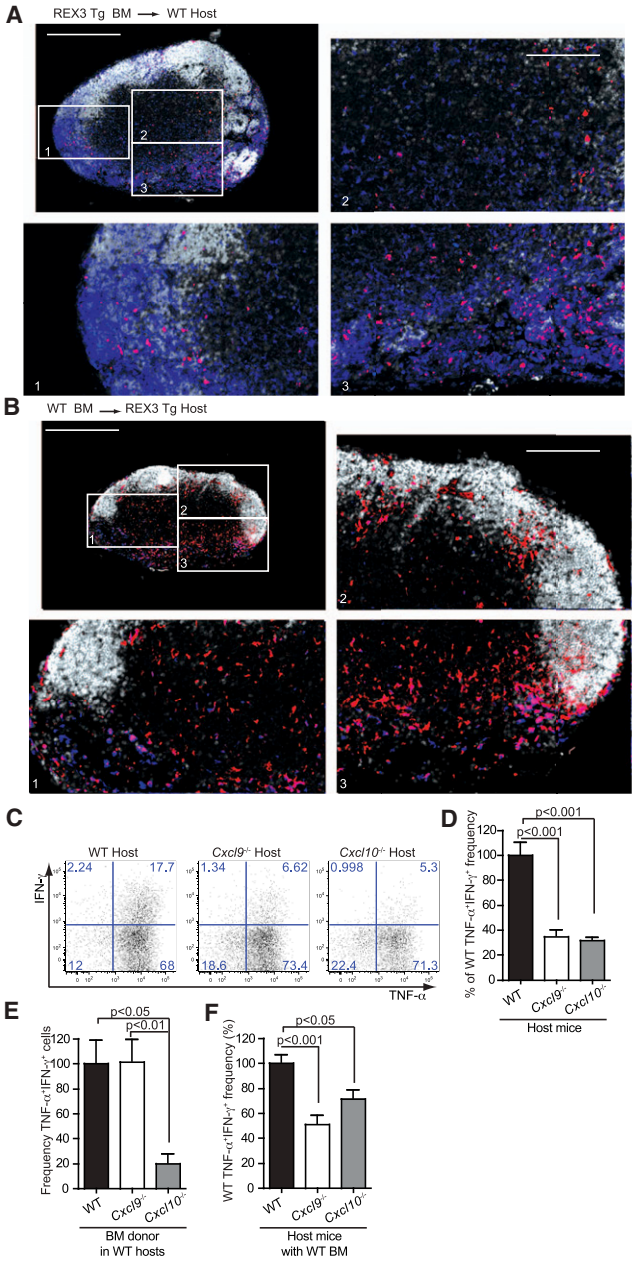

Figure 5. CXCL9 and CXCL10 Have Nonredundant Roles in Promoting OT-II Cell IFN-γ Responses after Host Immunization

(A and B) BM chimeras created with (A) REX3 Tg BM into WT hosts and (B) WT BM into REX3 Tg hosts. Reconstituted mice were immunized and transferred with OT-II cells. 24–36 hr after T cell transfer, dLNs reporter protein expression (CXCL9-RFP, red; CXCL10-BFP, blue; B220 and CD19 immunostaining, white). Scale bars represent 500 μm. Higher magnification images are from regions indicated (1, 2, 3).

(C) WT, *Cxcl9*$^{-/-}$, and *Cxcl10*$^{-/-}$ host mice were immunized into the footpad 24 hr prior to adoptive transfer of WT OT-II cells. At 60 hr after T cell transfer, dLNs were harvested and restimulated to assess cytokine production. Plots of IFN-γ and TNF-α production by WT OT-II cells transferred into WT, *Cxcl9*$^{-/-}$, or *Cxcl10*$^{-/-}$ hosts.

(D) Frequency of TNF-α$^+$IFN-γ$^+$ transferred OT-II cells in WT (black), *Cxcl9*$^{-/-}$ (open), and *Cxcl10*$^{-/-}$ (gray) hosts 60 hr after immunization.

(E) BM chimeras of WT hosts reconstituted with WT (black), *Cxcl9*$^{-/-}$ (open), *Cxcl10*$^{-/-}$ (gray) BM. Chimeras were immunized and transferred with WT OT-II cells. At 60 hr after T cell transfer, dLNs were harvested to assess cytokine production. Fold change of frequency of TNF-α$^+$IFN-γ$^+$ transferred cells in indicated BM chimeras is shown.

(F) BM chimeras of WT (black), *Cxcl9*$^{-/-}$ (open), *Cxcl10*$^{-/-}$ (gray) hosts reconstituted with WT BM. As in (E), dLN cytokine production. Fold change of frequency of TNF-α$^+$IFN-γ$^+$ transferred cells in indicated BM chimeras is shown.

Data are representative of two to three independent experiments (n = 4–8). Error bars denote SD.

findings suggest that a chemokine-dependent loop exists between priming CD4$^+$ T cells and antigen-presenting DCs, because expression of CXCL9 and CXCL10 was increased in LNs that received antigen-specific T cells. By tracking REX3^{2+} chemokine-expressing DCs, we have shown that they have higher expression of the activation markers CD86 and CD40. Signaling through CD40 has been shown to increase the expression of CXCL10 by DCs, and CD40L is increased on CXCR3-expressing T cells, indicating that this chemokine pathway may be important for the licensing of DCs during CD4$^+$ T cell priming (Quezada et al., 2004). Alternatively, the upregulation of CXCL10 may be through the production of type I and/or type II IFNs produced by antigen-presenting DCs themselves, transferred T cells, or by accessory cells, such as NK cells or pDCs, required for CD4$^+$ Th1 cell effector differentiation (Cervantes-Barragan et al., 2012; Martín-Fontecha et al., 2004).

We have shown that this chemokine-dependent loop between priming CD4$^+$ T cells and antigen-presenting DCs leads to differences in the intranodal behavior of CXCR3-competent and *Cxcr3*-deficient T cells during the second phase of T cell priming, which is important for T cell IFN-γ production (Hugues, 2010). *Cxcr3*$^{-/-}$ OT-II cells formed fewer and shorter interactions with CXCL10$^+$ (REX3$^+$) DCs, indicating that CXCL10-dependent tethering is important for T cell outcome. Interestingly, this difference appeared to occur prior to the massive upregulation of CXCR3 surface on WT OT-II cells, suggesting either that initial upregulation of CXCR3 was not detected by flow cytometry because of receptor internalization or that the low basal expression of CXCR3 expression by naive WT cells was important for this phenotype (Rabin et al., 1999). Along with increasing the tethering of DCs to T cells, CXCL10-CXCR3 interactions may also increase synapse formation, facilitating productive communication between these cells (Friedman et al., 2006; Molon et al., 2005). CXCR3 has been shown to be upregulated in vitro during the differentiation of multiple CD4$^+$ T cell lineages (Rabin et al., 2003; Sallusto et al., 1998); therefore, it may be that CXCR3 is required for all CD4$^+$ effector T cells, or that generation of other Th cell subsets have unique spatial requirements in the reactive LN that are controlled by other chemokine systems.

Our study has also established the concept that the location of T cells within the LN is important for specific Th cell polarization and that intranodal positioning of T cells is controlled, at least in part, by intranodal chemokine gradients. We found that CD4$^+$ T cells move out of the T cell zone to the outer LN after initial activation and upregulation of CXCR3 and that this process is controlled by CXCR3 ligands, which are induced predominantly in these peripheral regions of the LN. Recent studies have demonstrated that CD169$^+$ macrophages and other APCs

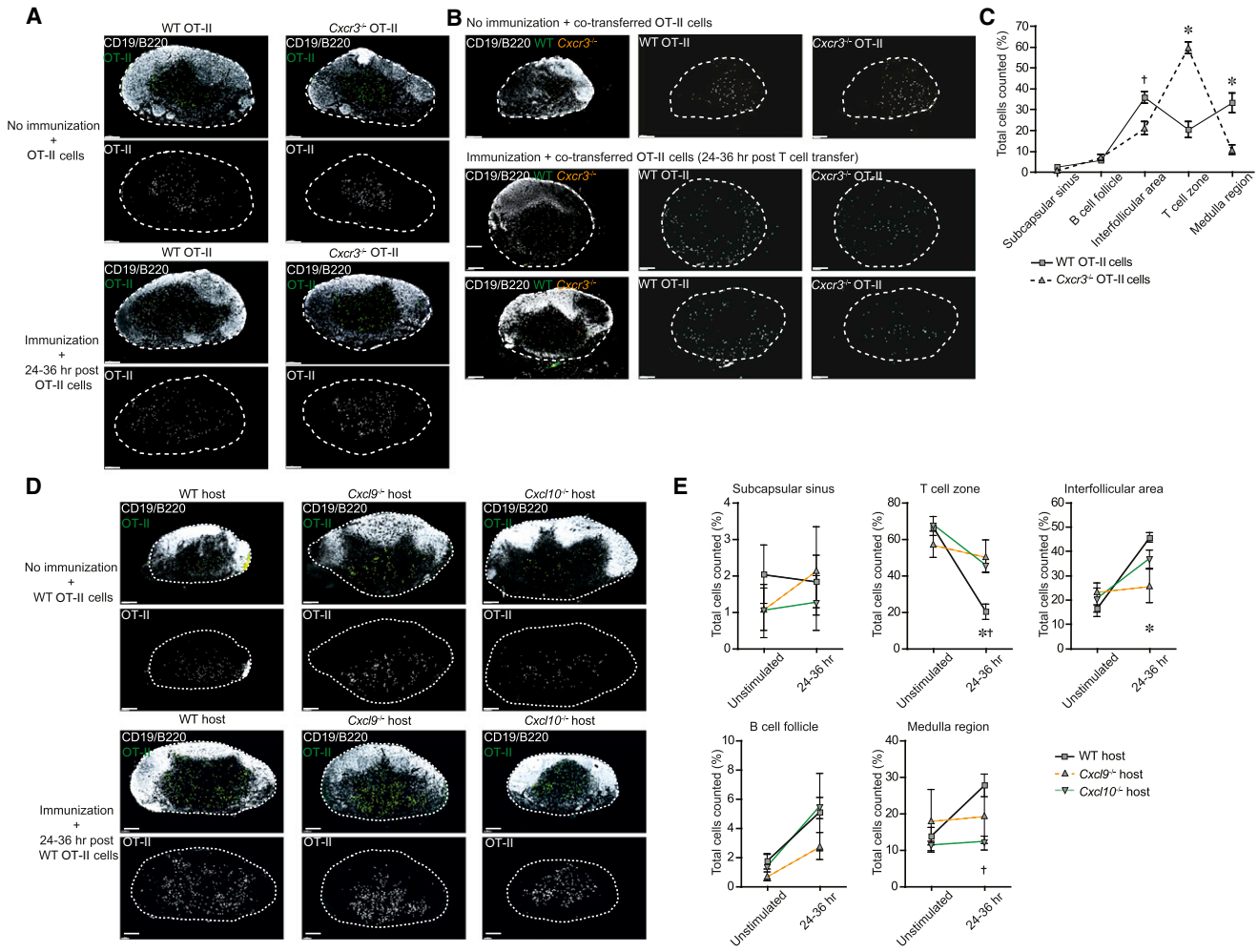

Figure 6. CXCR3 Ligands Determine Intranodal Location of Newly Activated OT-II Cells after Immunization

(A) Immunized and unimmunized WT hosts received Actin-GFP WT or *Cxcr3*$^{-/-}$ OT-II cells. T cell location 24–36 hr after T cell transfer.

(B and C) Unimmunized (top) and immunized (bottom; two representative LNs shown) WT hosts received cotransferred labeled WT (CMTMR, orange) and *Cxcr3*$^{-/-}$ (CMFDA, green) OT-II cells. T cell location 24–36 hr after T cell transfer. Regions of LN were determined as indicated in Figure S5.

(B) Representative snapshots of WT and *Cxcr3*$^{-/-}$ location in dLNs.

(C) Quantification of WT and *Cxcr3*$^{-/-}$ OT-II cell location in dLNs 24–36 hr after T cell transfer. †$p < 0.05$; *$p < 0.001$ between WT and *Cxcr3*$^{-/-}$ OT-II cells.

(D and E) Immunized and unimmunized WT, *Cxcl9*$^{-/-}$, and *Cxcl10*$^{-/-}$ hosts received transferred WT Actin-GFP OT-II cells. T cell location 24–36 hr after T cell transfer.

(D) Representative snapshots of WT and *Cxcr3*$^{-/-}$ location in dLNs.

(E) Quantification of WT OT-II cell locations in indicated hosts with and without immunization. *$p < 0.05$ between WT and *Cxcl9*$^{-/-}$ hosts; †$p < 0.05$ between WT and *Cxcl10*$^{-/-}$ hosts.

Scale bars represent 200 μm. Error bars denote SD.

present in the subcapsular sinus (SCS) and the interfollicular and medulla regions of dLNs efficiently trap antigen after lymph-borne viral challenge (Hickman et al., 2008; Iannacone et al., 2010). Importantly, loss of these macrophages results in reduced type I IFN production, suggesting a potential stimulus for CXCL9 and CXCL10 production after infection (Iannacone et al., 2010). Therefore, CXCR3 upregulation by recently activated T cells allows them to move to areas where they are poised to interact with antigen-presenting SCS macrophages or DC subsets, potentially providing T cells increased antigen stimulation and/or unique cytokine signals (Hickman et al., 2008).

Several studies have indicated the importance for CD8$^+$ T cells to leave the T cell zone and migrate into peripheral LN areas to interact with pathogen-loaded APCs (Hickman et al., 2008). Our study has expanded on these findings indicating that this process of intranodal relocation is also important for the development of Th1 CD4$^+$ cells. In addition, we now have shown that this movement is regulated by the ligands for CXCR3, and with the REX3 Tg mouse, we have identified the location and cell types expressing the chemokines responsible for this redistribution. Thus, our data suggest that the CXCR3 chemokine system is a key mediator of T cell peripheralization in the reactive

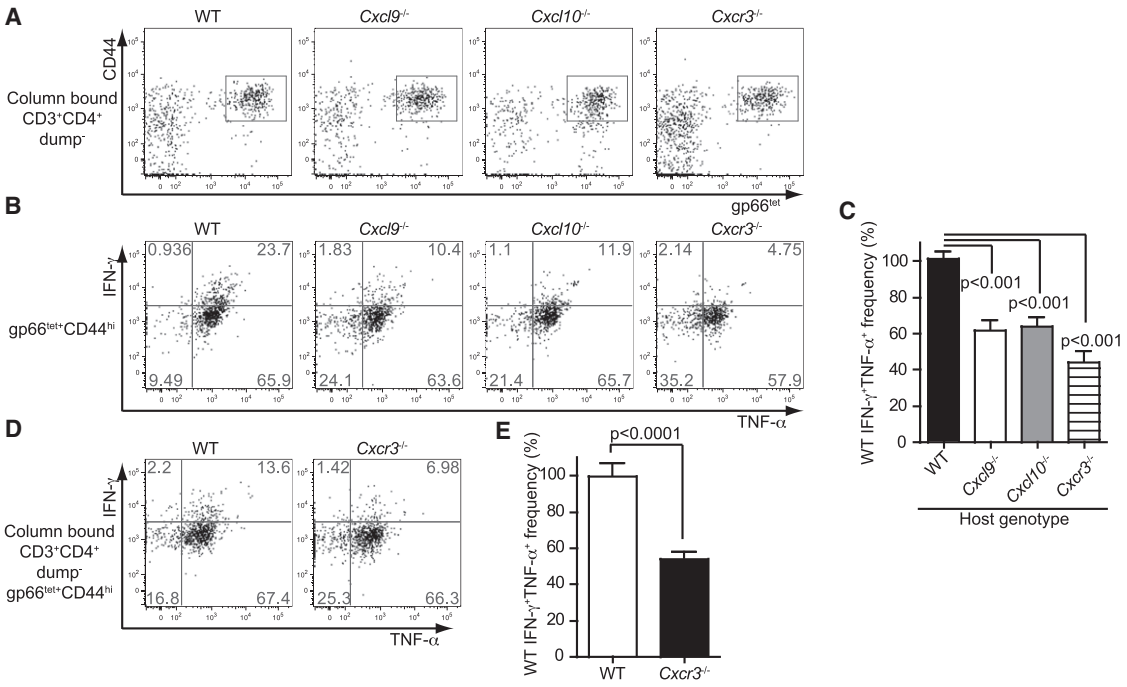

Figure 7. CXCR3 Is Required for Maximal Endogenous Antigen-Specific Th1 Cell Differentiation during Infection

(A–C) 8 days after i.v. LCMV infection, splenocytes from mice were harvested, restimulated, and tetramer enriched for detection of (A) LCMV gp66 tetramer-specific cells and (B, C) IFN-γ and TNF-α production.

(D and E) BM chimeras of mixed WT and *Cxcr3*$^{-/-}$ BM in *Rag1*$^{-/-}$ hosts were infected with LCMV and harvested for detection of IFN-γ and TNF-α production from LCMV-tetramer-positive cells.

Data are representative of two independent experiments (n = 4). Error bars denote SD.

LN after infection and immunization. Because CXCL10 is induced by TLRs and type I interferon, our data offer an explanation for why pathogen-activated macrophages and DCs in the LN periphery produce CXCL10 leading to the subsequent peripheralization of T cells. Further, as has been demonstrated in peripheral tissue (Groom and Luster, 2011a; Nakanishi et al., 2009), IFN-γ brought to these regions by early T cell emigrants probably amplifies the recruitment signal through the induction of CXCL9 and more CXCL10.

Because *Cxcr3* is a direct transcriptional target of T-bet (*Tbx21*), it is likely that our findings extend to cell fate decisions between effector and memory differentiation. Recently, CD4$^+$ T cells lacking T-bet have been described to preferentially differentiate into memory cells (Marshall et al., 2011; Pepper et al., 2011). Our study offers an explanation for these findings, suggesting that T-bet-dependent CXCR3 expression predisposes cells to become effector CD4$^+$ Th1 cells, as opposed to memory cells. Similar observations have recently been made for CD8$^+$ T cells where *Cxcr3*-deficient CD8$^+$ T cells locate to different areas of the spleen and preferentially become memory cells over effectors (Hu et al., 2011; Kohlmeier et al., 2011; Kurachi et al., 2011).

Our findings thus demonstrate unique spatial requirements for CD4$^+$ T cells during differentiation, which could have important implications in the design of potent Th1 cell-inducing vaccines. Our results, as well as the tools used to obtain them, lay the foundation for future studies aimed at identifying other factors that regulate Th1 cell responses in dLNs and peripheral inflamed tissues and at assessing the importance of the CXCR3 chemokine system in T cell fate decisions. Indeed, the development of the REX3 Tg mouse should be a valuable tool for the analysis of productive immune responses against infectious pathogens and for the rational design and analysis of vaccines.

EXPERIMENTAL PROCEDURES

Mice

C57BL/6 (BL/6), *CD90.1*, and OT-II mice were obtained from Jackson Laboratory. REX3 Tg mice in the C57BL/6 background were generated in our laboratory. All mice, including *Cxcr3*$^{-/-}$ (Hancock et al., 2000), *Cxcl9*$^{-/-}$ (Park et al., 2002), and *Cxcl10*$^{-/-}$ (Dufour et al., 2002) mice in the C57BL/6 background were housed under specific-pathogen-free conditions. All infectious work was performed in designated BL2$^+$ workspaces. All procedures were approved by the Massachusetts General Hospital Subcommittee on Research and Animal Care or by Harvard Committee on Microbiological Safety. See Supplemental Experimental Procedures for details of other mouse strains used.

Cell Preparation and Immunizations

DCs were CD11c$^+$ purified (Miltenyi) from mice implanted with Flt-3L B16 cells and pulsed with 10 μM OVA protein (Worthington) for 1 hr prior to 1 μg/ml LPS and poly(I:C) (InvivoGen) for another 1 hr. Tracked cells were labeled for 15 min at 37°C with 2 μM chloromethylfluorescein diacetate (CMFDA; Molecular Probes) prior to injection of 5 × 10^5 DCs into the footpad. Mice were immunized with 20 μg/ml OVA with 1 ng/ml LPS and poly(I:C). 24 hr after DC transfer or immunization, mice were given immunomagnetic selected 5 × 10^6 CD4$^+$ CD62L$^+$ (Miltenyi) T cells prepared from OT-II mice. To synchronize T cell responses, animals received 100 μg CD62L monoclonal antibody Mel-14 (100 μg per mouse; BioXcell). To block T cell egress, 1 mg/kg FTY720 (Cayman

Chemicals) was given i.p. 12 hr after T cell transfer. For imaging and localization experiments, transferred cells were either labeled with CMFDA or CMTRA as above, or alternatively Actin-GFP or Actin-RFP crossed to OT-II Tg mice were used.

Generation of REX3 Tg Mice

Targeting constructs for *Cxcl9*-RFP and *Cxcl10*-BFP were inserted into the RP24-164O11 BAC (CHORI), which contained the *Cxcl9* and *Cxcl10* genes. See Supplemental Experimental Procedures for details.

Cell Isolation and Flow Cytometry

Popliteal (draining) and brachial (nondraining) LNs were harvested, pooled, and massaged with tweezers to single-cell suspensions. For staining antibodies, see Supplemental Experimental Procedures. For analysis of polyfunctional T cell responses, cells were incubated with 20 μg/ml OVA (323–339) peptide (Peptides International) and 2 μg/ml αCD28 (Biolegend). After 1 hr, 10 μg/ml Brefeldin A (GolgiPlug; BD Biosciences) was added for an additional 3 hr. After surface staining, cells were fixed and permeabilized with Fix&Perm kit (Invitrogen) and stained for intracellular cytokines. Cells were resuspended in FACS buffer (2% FCS in PBS) and acquired on an LSR Fortessa flow cytometer (BD Biosciences) and analyzed with FlowJo software (Tree Star).

Immunofluorescence Staining

LNs were harvested into PLP buffer (0.05 M phosphate buffer containing 0.2 M L-lysine [pH 7.4], 2 mg/ml $NaIO_4$, 10 mg/ml paraformaldehyde), fixed for 5–12 hr, and dehydrated in 30% sucrose prior to embedding in OCT freezing media (Sakura Fineteck). 16 μm frozen sections were cut on a CM3050S cryostat (Leica). Sections were blocked in PBS containing 0.1% Triton X-100 (Sigma) and 10% goat serum (Jackson Immunoresearch) and stained in PBS (0.01% Triton X-100 and 5% goat serum). Images were acquired on a LSM510 confocal microscope (Carl Zeiss Mircoimaging). T cell regions were identified and labeled via immunostaining of B cell follicles and LN architecture, as described in Figure S5. Regions and cells were defined with IMARIS image analysis software (Bitplane), and center point spots were included in snapshot images.

LCMV Infection and Detection of gp66$^+$ Tetramer-Positive Cells

Mice were given 10^4 focus forming units of (Armstrong) LCMV i.v. 8 days prior to harvest. Splenocytes from LCMV-infected mice were restimulated with gp61-80 (AnaSpec) for 4 hr in the presence of Brefeldin A. Tetramer$^+$ cells were labeled with PE-gp66 tetramer for 1 hr and enriched with anti-PE magnetic microbeads (Moon et al., 2007).

Multiphoton Intravital Microscopy and Image Analysis

Performed as previously described (Mempel et al., 2004) and in Supplemental Experimental Procedures.

Statistical Analysis

Paired two-tailed Student's t tests were used for data analysis and generation of p values, for experiments when T cells from WT and *Cxcr3*$^{-/-}$ OT-II T cells were cotransferred (GraphPad Software). ANOVA via post-tukey test for multiple comparisons was used for experiments comparing more than two samples. p is shown for all significant ($p < 0.05$) analyses. All data are represented as mean with individual data points representing individual samples and time course data show mean with standard error of the mean (SEM) error bars. Bar graph data show standard deviation error (SD) bars.

SUPPLEMENTAL INFORMATION

Supplemental Information includes Supplemental Experimental Procedures, five figures, and one movie and can be found with this article online at http://dx.doi.org/10.1016/j.immuni.2012.08.016.

ACKNOWLEDGMENTS

Work was supported by the NIH grants CA069212 (to A.D.L.) and AI078897 (to U.H.v.A.). J.R.G. was supported by the NH&MRC, Australia (Fellowship 516791). J.H.S. was supported by a Samsung Scholarship. We thank D. Alvarez for assistance with LCMV infections, J. Farber for the *Cxcl9*$^{-/-}$ breeding pair, and C. Gerard for the *Cxcr3*$^{-/-}$ breeding pair.

Received: June 6, 2012
Accepted: August 29, 2012
Published online: November 1, 2012

REFERENCES

Bromley, S.K., Mempel, T.R., and Luster, A.D. (2008). Orchestrating the orchestrators: chemokines in control of T cell traffic. Nat. Immunol. *9*, 970–980.

Celli, S., Garcia, Z., and Bousso, P. (2005). CD4 T cells integrate signals delivered during successive DC encounters in vivo. J. Exp. Med. *202*, 1271–1278.

Cervantes-Barragan, L., Lewis, K.L., Firner, S., Thiel, V., Hugues, S., Reith, W., Ludewig, B., and Reizis, B. (2012). Plasmacytoid dendritic cells control T-cell response to chronic viral infection. Proc. Natl. Acad. Sci. USA *109*, 3012–3017.

Dufour, J.H., Dziejman, M., Liu, M.T., Leung, J.H., Lane, T.E., and Luster, A.D. (2002). IFN-gamma-inducible protein 10 (IP-10; CXCL10)-deficient mice reveal a role for IP-10 in effector T cell generation and trafficking. J. Immunol. *168*, 3195–3204.

Friedman, R.S., Jacobelli, J., and Krummel, M.F. (2006). Surface-bound chemokines capture and prime T cells for synapse formation. Nat. Immunol. *7*, 1101–1108.

Gattass, C.R., King, L.B., Luster, A.D., and Ashwell, J.D. (1994). Constitutive expression of interferon gamma-inducible protein 10 in lymphoid organs and inducible expression in T cells and thymocytes. J. Exp. Med. *179*, 1373–1378.

Groom, J.R., and Luster, A.D. (2011a). CXCR3 in T cell function. Exp. Cell Res. *317*, 620–631.

Groom, J.R., and Luster, A.D. (2011b). CXCR3 ligands: redundant, collaborative and antagonistic functions. Immunol. Cell Biol. *89*, 207–215.

Hancock, W.W., Lu, B., Gao, W., Csizmadia, V., Faia, K., King, J.A., Smiley, S.T., Ling, M., Gerard, N.P., and Gerard, C. (2000). Requirement of the chemokine receptor CXCR3 for acute allograft rejection. J. Exp. Med. *192*, 1515–1520.

Hickman, H.D., Takeda, K., Skon, C.N., Murray, F.R., Hensley, S.E., Loomis, J., Barber, G.N., Bennink, J.R., and Yewdell, J.W. (2008). Direct priming of antiviral CD8+ T cells in the peripheral interfollicular region of lymph nodes. Nat. Immunol. *9*, 155–165.

Hu, J.K., Kagari, T., Clingan, J.M., and Matloubian, M. (2011). Expression of chemokine receptor CXCR3 on T cells affects the balance between effector and memory CD8 T-cell generation. Proc. Natl. Acad. Sci. USA *108*, E118–E127.

Hugues, S. (2010). Dynamics of dendritic cell-T cell interactions: a role in T cell outcome. Semin. Immunopathol. *32*, 227–238.

Iannacone, M., Moseman, E.A., Tonti, E., Bosurgi, L., Junt, T., Henrickson, S.E., Whelan, S.P., Guidotti, L.G., and von Andrian, U.H. (2010). Subcapsular sinus macrophages prevent CNS invasion on peripheral infection with a neurotropic virus. Nature *465*, 1079–1083.

Ingulli, E., Mondino, A., Khoruts, A., and Jenkins, M.K. (1997). In vivo detection of dendritic cell antigen presentation to CD4(+) T cells. J. Exp. Med. *185*, 2133–2141.

Itano, A.A., McSorley, S.J., Reinhardt, R.L., Ehst, B.D., Ingulli, E., Rudensky, A.Y., and Jenkins, M.K. (2003). Distinct dendritic cell populations sequentially present antigen to CD4 T cells and stimulate different aspects of cell-mediated immunity. Immunity *19*, 47–57.

Kohlmeier, J.E., Reiley, W.W., Perona-Wright, G., Freeman, M.L., Yager, E.J., Connor, L.M., Brincks, E.L., Cookenham, T., Roberts, A.D., Burkum, C.E., et al. (2011). Inflammatory chemokine receptors regulate CD8(+) T cell contraction and memory generation following infection. J. Exp. Med. *208*, 1621–1634.

Kurachi, M., Kurachi, J., Suenaga, F., Tsukui, T., Abe, J., Ueha, S., Tomura, M., Sugihara, K., Takamura, S., Kakimi, K., and Matsushima, K. (2011). Chemokine receptor CXCR3 facilitates CD8(+) T cell differentiation into short-lived effector cells leading to memory degeneration. J. Exp. Med. *208*, 1605–1620.

Marshall, H.D., Chandele, A., Jung, Y.W., Meng, H., Poholek, A.C., Parish, I.A., Rutishauser, R., Cui, W., Kleinstein, S.H., Craft, J., and Kaech, S.M. (2011). Differential expression of Ly6C and T-bet distinguish effector and memory Th1 CD4(+) cell properties during viral infection. Immunity *35*, 633–646.

Martín-Fontecha, A., Thomsen, L.L., Brett, S., Gerard, C., Lipp, M., Lanzavecchia, A., and Sallusto, F. (2004). Induced recruitment of NK cells to lymph nodes provides IFN-gamma for T(H)1 priming. Nat. Immunol. *5*, 1260–1265.

Matloubian, M., Lo, C.G., Cinamon, G., Lesneski, M.J., Xu, Y., Brinkmann, V., Allende, M.L., Proia, R.L., and Cyster, J.G. (2004). Lymphocyte egress from thymus and peripheral lymphoid organs is dependent on S1P receptor 1. Nature *427*, 355–360.

Mempel, T.R., Henrickson, S.E., and Von Andrian, U.H. (2004). T-cell priming by dendritic cells in lymph nodes occurs in three distinct phases. Nature *427*, 154–159.

Miller, M.J., Safrina, O., Parker, I., and Cahalan, M.D. (2004). Imaging the single cell dynamics of CD4+ T cell activation by dendritic cells in lymph nodes. J. Exp. Med. *200*, 847–856.

Molon, B., Gri, G., Bettella, M., Gómez-Moutón, C., Lanzavecchia, A., Martínez-A, C., Mañes, S., and Viola, A. (2005). T cell costimulation by chemokine receptors. Nat. Immunol. *6*, 465–471.

Moon, J.J., Chu, H.H., Pepper, M., McSorley, S.J., Jameson, S.C., Kedl, R.M., and Jenkins, M.K. (2007). Naive CD4(+) T cell frequency varies for different epitopes and predicts repertoire diversity and response magnitude. Immunity *27*, 203–213.

Moon, J.J., Dash, P., Oguin, T.H., 3rd, McClaren, J.L., Chu, H.H., Thomas, P.G., and Jenkins, M.K. (2011). Quantitative impact of thymic selection on Foxp3+ and Foxp3- subsets of self-peptide/MHC class II-specific CD4+ T cells. Proc. Natl. Acad. Sci. USA *108*, 14602–14607.

Nakanishi, Y., Lu, B., Gerard, C., and Iwasaki, A. (2009). CD8(+) T lymphocyte mobilization to virus-infected tissue requires CD4(+) T-cell help. Nature *462*, 510–513.

Obst, R., van Santen, H.M., Mathis, D., and Benoist, C. (2005). Antigen persistence is required throughout the expansion phase of a CD4(+) T cell response. J. Exp. Med. *201*, 1555–1565.

Oxenius, A., Bachmann, M.F., Ashton-Rickardt, P.G., Tonegawa, S., Zinkernagel, R.M., and Hengartner, H. (1995). Presentation of endogenous viral proteins in association with major histocompatibility complex class II: on the role of intracellular compartmentalization, invariant chain and the TAP transporter system. Eur. J. Immunol. *25*, 3402–3411.

Padovan, E., Spagnoli, G.C., Ferrantini, M., and Heberer, M. (2002). IFN-alpha2a induces IP-10/CXCL10 and MIG/CXCL9 production in monocyte-derived dendritic cells and enhances their capacity to attract and stimulate CD8+ effector T cells. J. Leukoc. Biol. *71*, 669–676.

Park, M.K., Amichay, D., Love, P., Wick, E., Liao, F., Grinberg, A., Rabin, R.L., Zhang, H.H., Gebeyehu, S., Wright, T.M., et al. (2002). The CXC chemokine murine monokine induced by IFN-gamma (CXC chemokine ligand 9) is made by APCs, targets lymphocytes including activated B cells, and supports antibody responses to a bacterial pathogen in vivo. J. Immunol. *169*, 1433–1443.

Pepper, M., Pagán, A.J., Igyártó, B.Z., Taylor, J.J., and Jenkins, M.K. (2011). Opposing signals from the Bcl6 transcription factor and the interleukin-2 receptor generate T helper 1 central and effector memory cells. Immunity *35*, 583–595.

Quezada, S.A., Jarvinen, L.Z., Lind, E.F., and Noelle, R.J. (2004). CD40/CD154 interactions at the interface of tolerance and immunity. Annu. Rev. Immunol. *22*, 307–328.

Rabin, R.L., Park, M.K., Liao, F., Swofford, R., Stephany, D., and Farber, J.M. (1999). Chemokine receptor responses on T cells are achieved through regulation of both receptor expression and signaling. J. Immunol. *162*, 3840–3850.

Rabin, R.L., Alston, M.A., Sircus, J.C., Knollmann-Ritschel, B., Moratz, C., Ngo, D., and Farber, J.M. (2003). CXCR3 is induced early on the pathway of CD4+ T cell differentiation and bridges central and peripheral functions. J. Immunol. *171*, 2812–2824.

Sallusto, F., Lenig, D., Mackay, C.R., and Lanzavecchia, A. (1998). Flexible programs of chemokine receptor expression on human polarized T helper 1 and 2 lymphocytes. J. Exp. Med. *187*, 875–883.

Sierro, F., Biben, C., Martínez-Muñoz, L., Mellado, M., Ransohoff, R.M., Li, M., Woehl, B., Leung, H., Groom, J., Batten, M., et al. (2007). Disrupted cardiac development but normal hematopoiesis in mice deficient in the second CXCL12/SDF-1 receptor, CXCR7. Proc. Natl. Acad. Sci. USA *104*, 14759–14764.

Tang, H.L., and Cyster, J.G. (1999). Chemokine up-regulation and activated T cell attraction by maturing dendritic cells. Science *284*, 819–822.

Varga, S.M., and Welsh, R.M. (2000). High frequency of virus-specific interleukin-2-producing CD4(+) T cells and Th1 dominance during lymphocytic choriomeningitis virus infection. J. Virol. *74*, 4429–4432.

Yoneyama, H., Narumi, S., Zhang, Y., Murai, M., Baggiolini, M., Lanzavecchia, A., Ichida, T., Asakura, H., and Matsushima, K. (2002). Pivotal role of dendritic cell-derived CXCL10 in the retention of T helper cell 1 lymphocytes in secondary lymph nodes. J. Exp. Med. *195*, 1257–1266.

Yoneyama, H., Matsuno, K., Zhang, Y., Nishiwaki, T., Kitabatake, M., Ueha, S., Narumi, S., Morikawa, S., Ezaki, T., Lu, B., et al. (2004). Evidence for recruitment of plasmacytoid dendritic cell precursors to inflamed lymph nodes through high endothelial venules. Int. Immunol. *16*, 915–928.

Zhu, J., Yamane, H., and Paul, W.E. (2010). Differentiation of effector CD4 T cell populations (*). Annu. Rev. Immunol. *28*, 445–489.